

Article

Monthly Variation in Mycosporine-like Amino Acids from Red Alga Dulse (*Devaleraea inkyuleei*, Formerly *Palmaria palmata* in Japan)

Ryuya Yamamoto ¹, Martin Alain Mune Mune ^{2,3}, Yoshikatsu Miyabe ^{1,4}, Hideki Kishimura ⁵ 
and Yuya Kumagai ^{5,*} 

¹ Chair of Marine Chemical Resource Development, Graduate School of Fisheries Sciences, Hokkaido University, Hakodate 041-8611, Hokkaido, Japan

² JSPS Postdoctoral Fellowship for Research in Japan, Graduate School of Fisheries Sciences, Hokkaido University, Hakodate 041-8611, Hokkaido, Japan

³ Faculty of Science, University of Maroua, Maroua P.O. Box 814, Cameroon

⁴ Aomori Prefectural Industrial Technology Research Center, Hachinohe 031-0831, Aomori, Japan

⁵ Laboratory of Marine Chemical Resource Development, Faculty of Fisheries Sciences, Hokkaido University, Hakodate 041-8611, Hokkaido, Japan

* Correspondence: yuyakumagai@fish.hokudai.ac.jp; Tel.: +81-138-40-5560

Abstract: Mycosporine-like amino acids (MAAs) are natural ultraviolet-absorbing compounds found in microalgae and macroalgae. MAA content changes seasonally and in response to environmental factors. We previously investigated MAAs from the red alga dulse (*Devaleraea inkyuleei*, formerly *Palmaria palmata* in Japan) in Usujiri, Hokkaido, Japan, from 2019 to 2020. At that time, some factors affecting MAA content were still unclear. In this study, we investigated MAA variation during the period from January to June 2021, and evaluated new methods of MAA extraction from dulse. We recorded a maximum MAA extraction yield (7.03 $\mu\text{mol/g}$ dry weight) on 25 March 2021. Over the course of our three years of investigations from 2019 to 2021, we found that dulse was most suitable for MAA preparation from the middle of February to late April. In the later work reported in this paper, we improved our extraction method by using a lower-risk organic solvent (ethanol) rather than methanol. In addition, we evaluated MAA extraction using different levels of ethanol concentration (25, 50, and 99%) and different extraction times (2, 6, and 24 h). We found that extraction with 25% ethanol for 24 h increased MAA content by a factor of 3.2, compared with our previous extraction method. In summary, we determined the most suitable sampling period for Usujiri dulse, to extract the highest content of MAAs. We also improved the effectiveness of the extraction process.

Keywords: red alga; dulse; mycosporine-like amino acids; monthly variation; extraction yield; chemical composition



check for updates

Citation: Yamamoto, R.; Mune Mune, M.A.; Miyabe, Y.; Kishimura, H.; Kumagai, Y. Monthly Variation in Mycosporine-like Amino Acids from Red Alga Dulse (*Devaleraea inkyuleei*, Formerly *Palmaria palmata* in Japan). *Phycology* **2023**, *3*, 127–137. <https://doi.org/10.3390/phycolgy3010008>

Academic Editor: Peer Schenk

Received: 24 December 2022

Revised: 31 January 2023

Accepted: 7 February 2023

Published: 9 February 2023



Copyright: © 2023 by the authors. Licensee MDPI, Basel, Switzerland. This article is an open access article distributed under the terms and conditions of the Creative Commons Attribution (CC BY) license (<https://creativecommons.org/licenses/by/4.0/>).

1. Introduction

Mycosporine-like amino acids (MAAs) are natural UV-absorbing compounds. In recent years, MAAs have attracted much attention for their application in cosmetics. Researchers have also investigated the antibacterial, anticancer, antiviral, and antiallergic properties of MAAs for pharmaceutical purposes [1–4]. However, interest in the application of MAAs has mainly focused on their ultraviolet protection qualities. Ultraviolet radiation (UVR) has harmful effects on human skin, including erythema, hyperpigmentation, photoaging, and skin cancer [5–7]. In this regard, the importance of sunscreen products to protect human skin has recently increased. Synthetic reagent products cause environmental issues such as coral bleaching [8]. For this reason, natural compounds with high molar extinction coefficients have been proposed as alternative UV protection agents [9].

The intensity of UVR reaching Earth has been gradually increasing due to a loss in the ozone layer [10]. Marine organisms in intertidal zones are exposed to sunlight;

therefore, they have evolved photoprotection mechanisms to protect themselves [11–13]. UVR induces reactive oxygen species (ROS) generation, and also causes oxidative stress and DNA damage. One means by which marine organisms such as seaweed, cyanobacteria, phytoplankton, and marine animals protect themselves involves the accumulation of MAAs as a UVR absorber [14–16].

MAAs, which are constituted by a core structure of cyclohexenone or cyclohexenimine rings, are secondary metabolites with a strong UVR absorption capacity. Depending on their molecular structures, the UV absorption maxima of MAAs range from 310 to 360 nm [17], and they have a high molar extinction coefficient ($\epsilon = 28,000\text{--}50,000$) [18–20]. This absorption range covers both UV-A (320–400 nm) and UV-B (280–320 nm) radiation. MAAs exhibit high water solubility, high stability, low toxicity, and antioxidant activity [21,22]. Low levels of MAA content are found in marine organisms because of their high molecular extinction coefficient. Among these organisms, red algae are regarded as one of the most abundant natural sources of MAAs, and have shown promise in the cosmetic industry for photoprotection purposes [23,24].

The chemical structures of MAAs in red algae vary among species and are affected by factors such as pH, temperature, irradiation, chlorophyll, phytoplankton, nutrients, water depth, and harvest time [25–28]. A positive correlation between strong solar radiation and MAA content has been reported [29]. Red algae in intertidal zones have a higher MAA content than species in subtidal zones. Researchers have also found that the MAA content of red algae in low-latitude zones is higher than that of algae in high-latitude areas [30,31]. MAAs in algae have also been shown to exhibit various resistance functions against environmental factors such as heat stress, osmoregulation, drying, and nitrogen storage [17,32–35]. However, MAA composition changes with changes in habitat, even within the same red algae species [36]. Findings such as these highlight the need to clarify the influence of environmental factors, so that MAAs may be more effectively used in industrial applications.

Kombu is an important resource in the city of Hakodate, on the northern Japanese island of Hokkaido. The red alga dulse (*Devaleraea inkyuleei* in Japan, formerly *Palmaria palmata* [37]) grows on Kombu rope and is regarded as an underused marine resource in the area. Attempts have been made to utilize dulse as a novel local food, and to evaluate its functions such as antioxidant activity [38,39]. It has also been studied as a source of peptides for the inhibition of angiotensin I-converting enzyme activity [40] and of xylooligosaccharides for prebiotics [41,42]. Dulse has also been the subject of genome analysis [43,44] and of pigment-containing protein structural analyses [45]. Our previous two-year investigation found that dulse contained MAAs as major UV absorption compounds [46,47], but compositional variations were still unclear at that time.

In this study, we investigated the monthly variations in MAA content in dulse collected from Usujiri, Hokkaido, in the first half of 2021, to clarify variations in MAA content. In addition, to reduce the risk of harmful organic solvent, we used ethanol as a low-risk solvent and sought to evaluate its effectiveness.

2. Materials and Methods

2.1. Algal Sample Preparation

All dulse samples (*Devaleraea inkyuleei* in Japan, formerly *Palmaria palmata* [37]) were collected at 1 m depth in Usujiri, Hakodate, Japan, from January to June 2021. Thalli were washed with tap water to remove sea salt and impurities. Lyophilized algal samples were ground into a fine powder using Wonder Blender WB-1 (Osaka Chemical Co., Osaka, Japan).

2.2. Extraction of Crude MAAs from Dulse

The extraction of MAAs from dulse was performed as in our previous studies [46,47]. One gram of fine powder sample was suspended in 20 mL of distilled water at 4 °C for 6 h. The water-soluble extract was then collected via centrifugation at 4 °C, 27,200 × g for

10 min. The supernatant was lyophilized and resolved in 20 mL of methanol at 4 °C for 2 h. MAAs were collected via centrifugation at 4 °C, 27,200 × *g* for 10 min. The supernatant was evaporated and dissolved in water, the solution was centrifuged, and the supernatant was lyophilized. Solid samples were then designated as crude MAAs and were used for experimental purposes.

2.3. HPLC Analysis of MAAs

The crude MAAs were dissolved in water containing 0.1% trifluoroacetic acid (TFA) and subjected to sequential filtration via Millex-GV (pore size: 0.22 μm) (Merck Millipore, Billerica, MA, USA) and Millex-LG (pore size: 0.20 μm) (Merck Millipore). The filtrated MAAs were isolated via reversed-phase HPLC using a Mightysil RP-18GP column (5 μm, 10 × 250 mm) (Kanto Kagaku, Tokyo, Japan), with the column oven set to 40 °C and a detection wavelength of 330 nm, and using an isocratic elution of pure water containing 0.1% TFA for 7 min, and a linear gradient of acetonitrile (0–70%) containing 0.1% TFA for 13 min, at a flow rate of 4.73 mL/min. MAA content was expressed in terms of molecules per gram of dry dulse powder (μmol/g DW (dry weight)). The lambda max of each MAA was identified using a spectrophotometer (UV-1800, Shimadzu, Kyoto, Japan) after separation via HPLC.

2.4. Protein, Phycoerythrin (PE), and Sugar Content

The amount of crude protein was determined gravimetrically. One gram of fine powder was dissolved in 20 mL water and extract at 4 °C for 12 h. After centrifugation at 12,000 × *g* for 5 min, the supernatant was dialyzed against water at 4 °C and lyophilized. For each sample, phycoerythrin (PE) was prepared from fine powders. A 10 mg amount of powder was dissolved in 1 mL distilled water and extracted at 4 °C for 12 h. After centrifugation at 12,000 × *g* for 5 min, the spectra of the supernatant were measured via the UV-visible ray absorption spectrum using a spectrophotometer (UV-1800, Shimadzu, Kyoto, Japan). The amount of PE was determined by the following equation [48]: PE (mg/mL) = [(A₅₆₄ − A₅₉₂) − (A₄₅₅ − A₅₉₂) × 0.2] × 0.12. Main sugar content was determined by detected amounts of glucose and xylose. Powder was hydrolyzed using trifluoro acid, and glucose and xylose contents were determined using a glucose assay kit (Fujifilm Wako Shibayagi, Gunma, Japan) and a D-xylose assay kit (Megazyme, Wicklow, Ireland), respectively.

2.5. Abiotic Data in Hakodate

Monthly means of the daily maximum ultraviolet index (UVI) were obtained from the Japan Meteorological Agency (JMA: https://www.data.jma.go.jp/gmd/env/uvhp/info_uv.html, accessed on 27 December 2021). Following the method recommended by the JMA, erythemal UV intensity (mW/m²) was calculated by multiplying UVI by a factor of 25. The data of near-surface chlorophyll concentrations (mg/m³) were obtained from NASA's Ocean Color WEB (<https://oceancolor.gsfc.nasa.gov>, accessed on 25 October 2021).

2.6. Compositional Comparison of Usujiri Dulse from 2019 to 2021

Data of MAAs from Usujiri dulse obtained between 2019 and 2020 were taken from our previous research [45,46]. Sampling of dulse growing at a depth of 1–2 m was performed in the same Usujiri area as was the case previously. Data of erythemal UVI and near-surface chlorophyll concentration in 2019 and 2020 were obtained from the JMA and from NASA's Ocean Color WEB.

2.7. Ethanol Extraction of MAAs

To evaluate the extraction effectiveness using an organic solvent that was low-risk to human health, extraction was performed using different concentrations of ethanol for different periods of time. One gram of powder was suspended in 20 mL of 25, 50, or 99% ethanol and extracted at 4 °C for 2, 6, or 24 h. The supernatant was collected via

centrifugation at 4 °C, 27,200× g for 10 min, and the composition of MAAs was evaluated via HPLC.

2.8. Statistical Analysis

Data are expressed as the mean ± standard error. All values are means of triplicate analysis. Statistical analysis was carried out using the Tukey–Kramer multiple comparisons test. All statistical analyses were performed using Statcel 3 software (Version No. 3, OMS Publisher, Tokorozawa, Japan).

3. Results and Discussion

3.1. Monthly Variations in MAAs from Usujiri Dulse in 2021

We extracted MAAs from dulse using the same method used in our previous research [46,47]. The 2021 extract contained six types of MAAs (shinorine, palythine, asterina-330, porphyra-334, usujirene, and palythene), as in 2019–2020. After separation via HPLC, these MAAs were identified by MALDI-TOF/MS or H-NMR [38,46]. The monthly variations are shown in Figure 1 and Supplementary Figure S1. Asterina-330 and shinorine were present only in small amounts. The main components were palythine and porphyra-334. The peaks of usujirene and palythene were not separated via HPLC [46,47], and their extinction coefficients were similar, as follows: usujirene, 45,070 M⁻¹ cm⁻¹; palythene, 47,521 M⁻¹ cm⁻¹. Therefore, we expressed the peak as usujirene + palythene and employed the extinction coefficient of palythene to avoid the risk of overestimation. The usujirene + palythene content was therefore the third largest. The total MAA content increased from January (2.95 µmol/g DW) to February (3.56 µmol/g DW), before peaking in March (7.03 µmol/g DW), and falling back sharply in April (3.83 µmol/g DW). MAA content was lowest in June (2.87 µmol/g DW). The content of porphyra-334 decreased significantly from March (2.96 µmol/g DW) to April (0.83 µmol/g DW). Palythine content did not change during the same period, but decreased from April (2.02 µmol/g DW) to June (1.42 µmol/g DW). Usujirene + palythene greatly decreased between March (1.53 µmol/g DW) and April (0.82 µmol/g DW) and then decreased slightly from April to June. These results showed that the composition of MAAs differed from month to month.

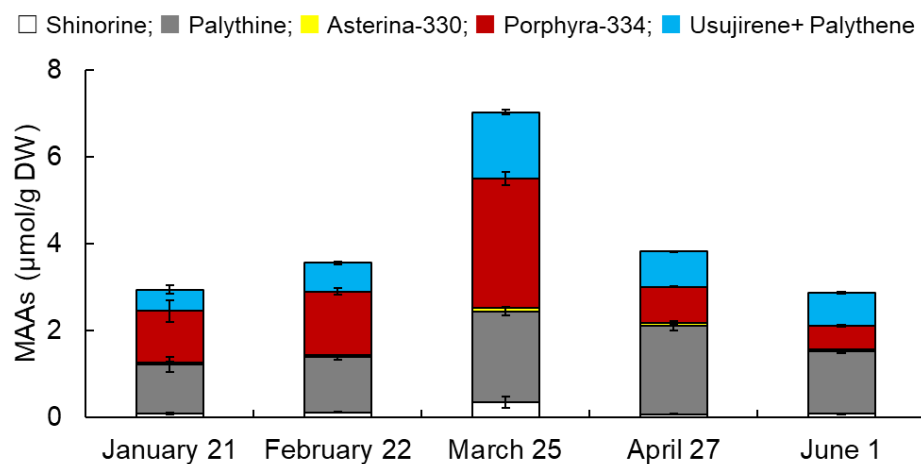


Figure 1. MAAs in 2021. The content of six MAAs—shinorine, palythine, asterina-330, porphyra-334, and usujirene + palythene—in dulse collected on 21 January, 22 February, 25 March, 27 April, and 1 June. Data show mean values, $n = 3$.

Comparing the 2021 data with those obtained for the previous past two years, we found a different result concerning palythene content, which increased from April to May in 2019 [46]. We observed that porphyra-334 and usujirene + palythene content decreased significantly from April to May in 2019 and 2020, as well as in 2021. However, in 2020,

palythene content decreased between March and April [47], one month earlier than in 2021. Finally, we found that MAA content changed from year to year even in the same sea area.

3.2. Monthly Variations in MAA Content

The molar percentages (mol%) of MAAs in 2021 were compared (Figure 2). The molar percentages of shinorine (a maximum of 5.0 mol% on 25 March and a minimum of 2.1 mol% on 27 April) and asterina-330 (a maximum of 2.1 mol% on 1 June and a minimum of 1.4 mol% on 25 March) were stable at low values. At the beginning of the study period, porphyra-334 was the major MAA, with approximately 41 mol% from 21 January to 25 March. This then decreased dramatically to 22 mol% on 27 April, with a further, smaller decrease to 19 mol% on 1 June. Palythine was more stable, at approximately 35 mol% until 25 March, and then became the major MAA with 51 mol% on 27 April. The mol% of usujirene + palythene increased gradually from 17 mol% on 21 January to 26 mol% on 25 March.

We found previously that the mol% of palythine increased from April to May in 2019 and 2020 [46,47]. The mol% of usujirene + palythene peaked in April before decreasing in May. Considering all three years of our investigations, we found that palythine replaced porphyra-334 as the major MAA in late April or early May.

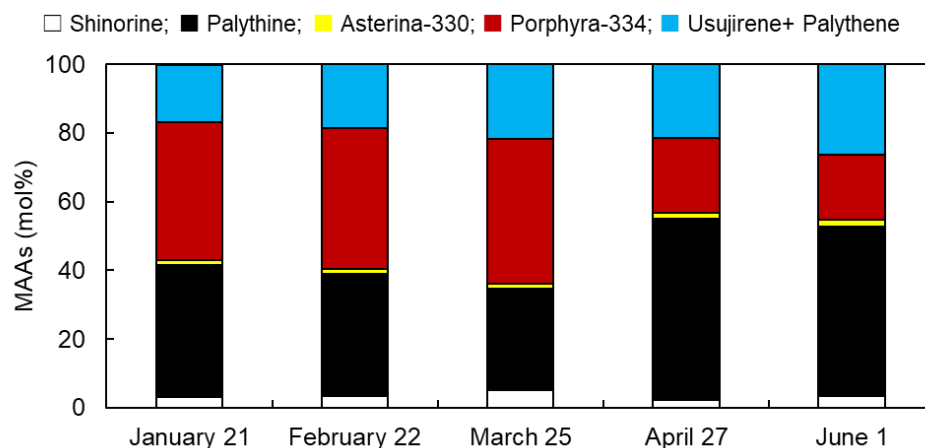


Figure 2. Molar percentages of MAAs in 2021. The content of six MAAs—shinorine, palythine, asterina-330, porphyra-334, and usujirene + palythene—in dulse collected on 21 January, 22 February, 25 March, 27 April, and 1 June. Data show mean values, $n = 3$.

3.3. Changes in MAAs, Proteins, Saccharides, and Erythematous UV Intensity

Our data showed that the content of MAAs changed monthly. We then examined the relationship between these variations and the composition of dulse (proteins and saccharides), and also with the environmental factor of erythematous UV intensity (Figure 3). Proteins and saccharides were the major components in dulse. The original components of acid hydrolysate containing glucose and xylose were floridean starch and xylan cell wall, respectively. Water-soluble protein and phycoerythrin (PE) content also followed the same trend. We designated water-soluble protein as protein, and PE was regarded as the main component of water-soluble protein. The amount of xylose increased gradually from January to June, while the protein amount decreased from March to June, suggesting that the increase in xylose was related to the decrease in protein. In addition, erythematous UV intensity increased constantly from January to June. The relationship between xylan and the UV protection function is not known. We hypothesized that dulse might protect itself from UVR by making a thick xylan cell wall, rather than by lowering MAA production in low nitrogen conditions. Interestingly, an increase in glucose was recorded between February and March, as well as an increase in MAAs. Floridean starch is a photosynthesis product, and an increase in sunlight in March might promote starch synthesis [49]. MAAs are biologically synthesized by the shikimate pathway and the pentose phosphate pathway,

which are also the routes of photosynthesis products [50]. However, the protein content of MAAs decreased in April. We hypothesized that the decrease in protein content would also include a decrease in starch synthase enzymes and in enzymes related to the shikimate and pentose phosphate pathways. Our results indicated that a decrease in MAAs corresponded to a decrease in floridean starch.

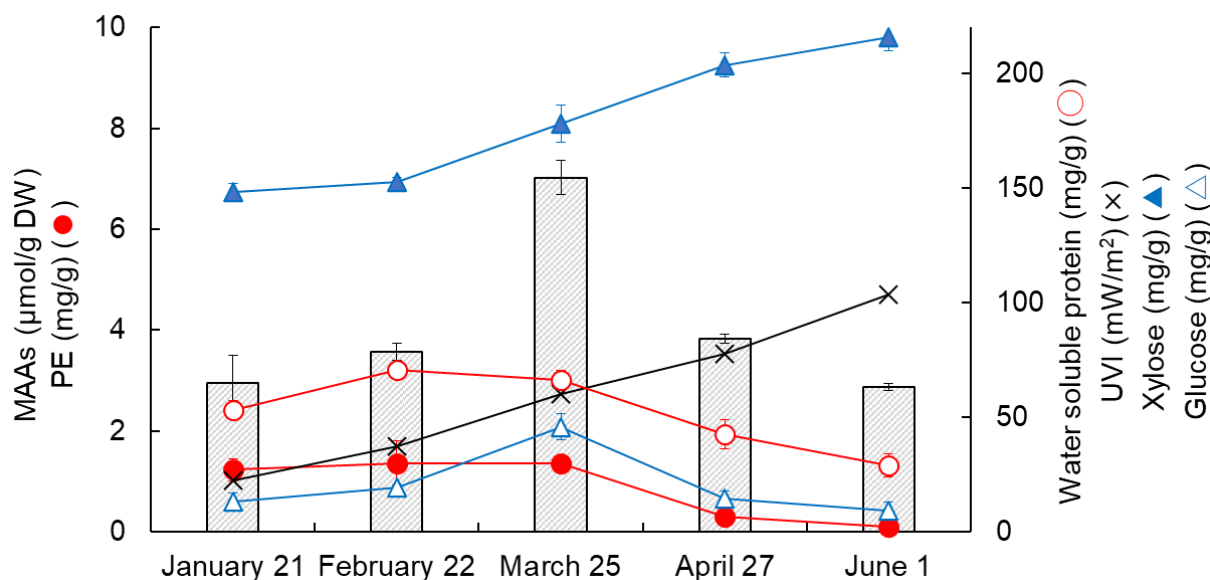


Figure 3. Monthly variations in MAAs, proteins, and saccharides in dulse collected in 2021. The amount of MAAs was expressed as total MAA content. Water-soluble protein was determined using the gravimetric method. The amount of PE from dry weight was determined using the Beer and Eshel equation [48]. Glucose and xylose were determined via colorimetric methods. Erythemal UV intensity was obtained from the Japan Meteorological Agency (https://www.data.jma.go.jp/gmd/env/uvhp/info_uv.html, accessed on 27 December 2021).

The amount of MAAs in red algae increased with erythemal UV intensity [51]. However, MAAs in dulse decreased from March to April. We collected data for erythemal UV intensity and chlorophyll concentration (from JMA and NASA's Ocean Color WEB) (Figure 4). An increase in chlorophyll concentration in the Usujiri area from January to June indicated a decrease in nitrogen sources due to the phytoplankton proliferation [52,53]. In addition to proteins, MAAs are also associated with nitrogen compounds in red algae [32,33]. For this reason, we previously concluded that a decrease in MAAs was associated with phytoplankton proliferation around the Usujiri area [46,47].

The amounts of MAAs and chlorophyll concentrations were also compared across the whole 2019–2021 study period. Although we found that chlorophyll concentrations differed from year to year, we also noted that the whole of Hokkaido was covered by a high concentration of chlorophyll in the March–April period in all years. This concentration then declined, beginning in the western part of Hokkaido. In 2020, this decrease in chlorophyll concentration was revealed in April, whereas in 2019 and 2021 it became apparent in May. These decreases resulted in a depletion of nutrients in the sea, so that the dulse was also lacking in nutrition, and this might have reduced its capacity for MAA synthesis. Although more surveys are needed to fully understand dulse composition, the results of our three years of study show that the most suitable period for sampling Usujiri dulse for MAA preparation extends from the middle of February to late April.

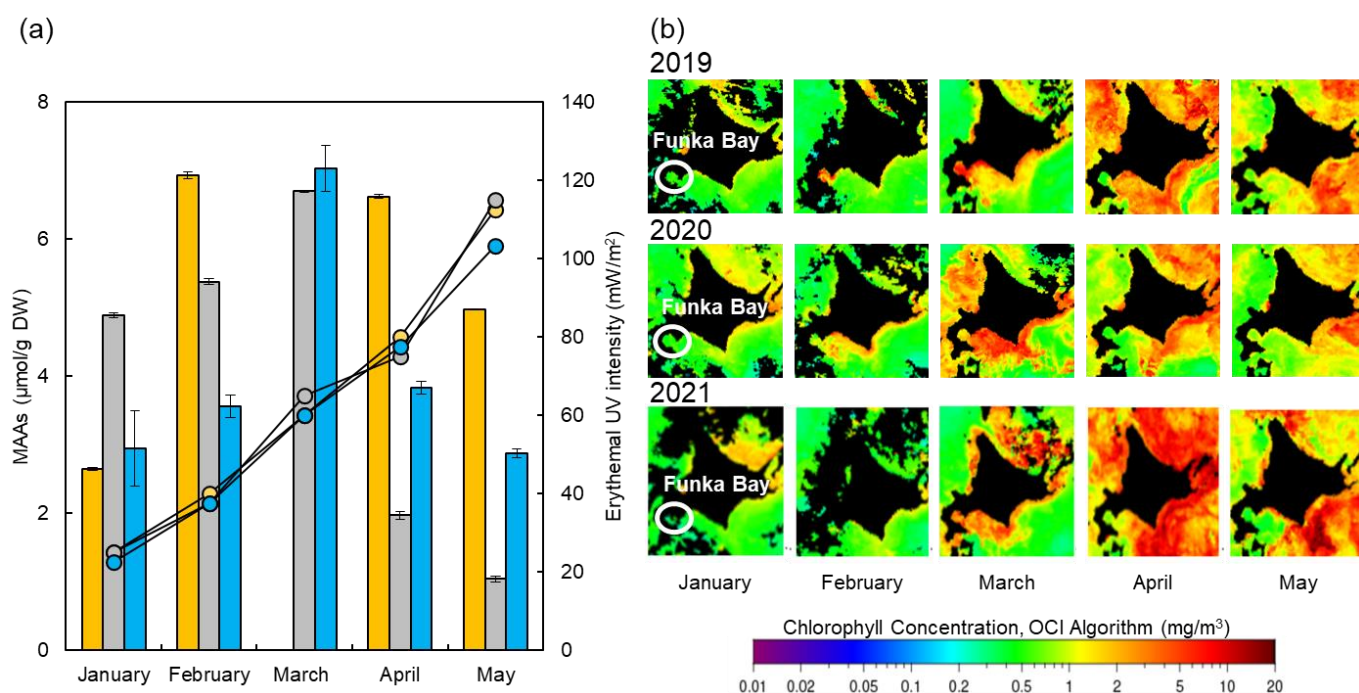


Figure 4. Monthly mean MAA contents, daily maximum erythemal UV intensities, and chlorophyll concentrations in 2019, 2020, and 2021. (a) MAA content and erythemal UV intensity. The orange bar and line show MAA content and erythemal UV intensity in 2019; the gray bar and line show MAA content and erythemal UV intensity in 2021; the blue bar and line show MAA content and erythemal UV intensity in 2021. (b) Chlorophyll concentrations. The sampling place was Usujiri, at the entrance to Funka Bay. These data were obtained from JMA and NASA’s Ocean Color WEB. All data were recorded in 2019–2021.

3.4. Evaluation of Ethanol Extraction of MAAs from Dulse

In our previous work, we employed the water–methanol successive extraction method for MAA extraction from dulse. In this study, to better consider the use of MAAs for industrial applications, we investigated extraction conditions using an alternative organic solvent—ethanol—which is safer than methanol. To this end, we used dulse powder from the 25 March 2021 sample and evaluated the effects of different ethanol concentrations (25, 50, and 99%) and extraction times (2, 6, and 24 h) (Figure 5a). We found that extraction with 99% ethanol produced a low yield of MAAs up to 24 h. For periods up to 6 h, extraction with 25 and 50% ethanol produced higher MAA yields than the water–methanol successive extraction method. Overall, a long extraction time (24 h) resulted in a yield of MAAs that was approximately 1.7 times higher than shorter periods (2 or 6 h). The most suitable condition involved extraction with 25% ethanol for 24 h. This resulted in an MAA yield of $22.7 \mu\text{mol/g DW}$, which was 3.2 times higher than the yield obtained using the water–methanol successive extraction method.

We also compared the composition of MAAs obtained using 25% ethanol for 24 h with those obtained by the water–methanol successive extraction method in terms of mol% (Figure 5b). The yields of palythine (28.3 mol%) and asterina-330 (1.3 mol%) in 25% ethanol extraction were equal to those in water–methanol successive extraction (29.7 mol% for palythine; 1.4 mol% for asterina-330). The mol% of shinorine in 25% ethanol extraction was 2.4 times higher. The mol% of Porphyra-334 in 25% ethanol extraction was slightly higher, while that of usujirene + palythene was considerably lower. Finally, the yield of usujirene + palythene with 25% ethanol extraction was 0.56 times the yield obtained by water–methanol successive extraction.

Usujirene + palythene have an absorption maximum of around 360 nm. This differs slightly from that of other MAAs which have absorption maxima of around 330 nm. We

previously evaluated the water extraction yield of MAAs [46]. The maximum absorption of around 360 nm increased as extraction time increased from 2 to 6 h, and then decreased with time dependently. Porphyra-334 is thought to be the precursor of usujirene + palythene, and usujirene + palythene was hydrolyzed, becoming palythine [46]. This finding suggested that usujirene + palythene was enzymatically synthesized from porphyra-334, accompanying the water extraction. The combined mol% values of porphyra-334 and usujirene + palythene were quite similar for both the 25% ethanol extraction and water–methanol successive extraction methods (58.3 and 63.9 mol%, respectively).

Other MAA extraction conditions such as 80% ethanol for 5 min and 25% methanol for 2 h have also been reported in the literature [54–56]. However, the evaluation of extraction conditions has been less well reported. In this study, we determined the most suitable ethanol concentration and extraction time for MAAs and also evaluated MAA composition. The information presented here should help to improve the efficiency of the MAA extraction process.

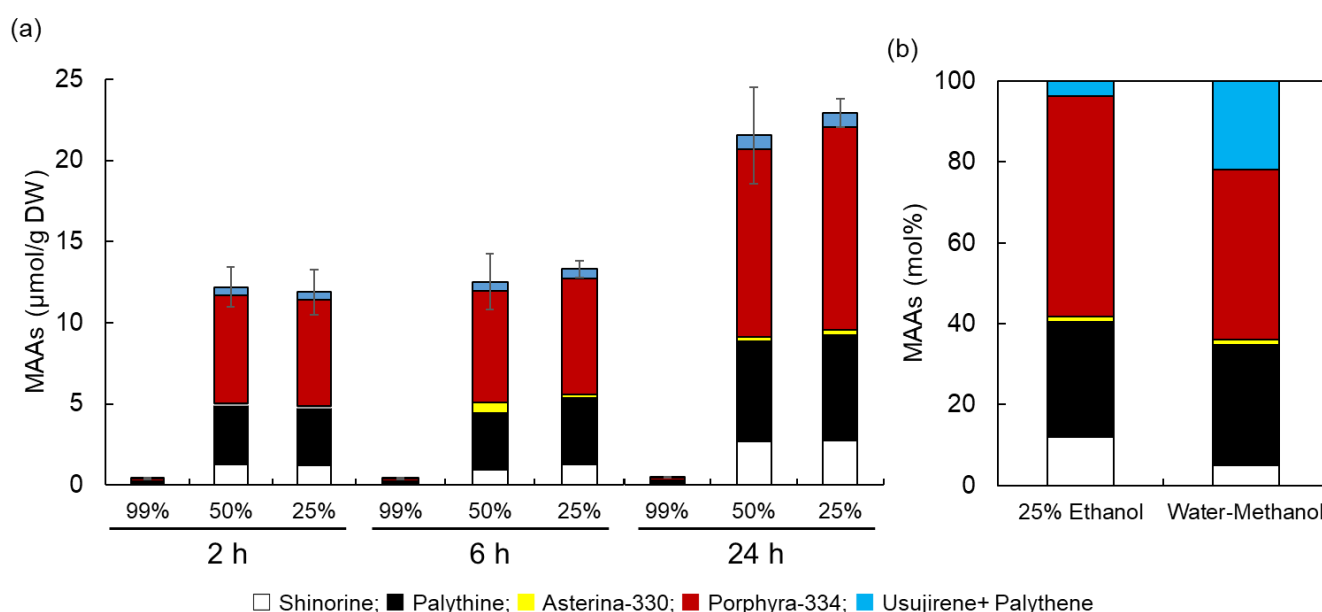


Figure 5. (a) Effects of different ethanol concentrations and extraction times on MAA yields. Three ethanol concentrations (25, 50, and 99%) and three extraction times (2, 6, and 24 h) were evaluated. Concentrations of each MAA were detected via HPLC. Error bars show the average of total MAAs ($n = 3$). (b) Molar percentages of MAAs obtained using different extraction methods. Data were obtained from dulse collected on 25 March 2021. The data show mean values, $n = 3$. The values of 100 mol% in 25% ethanol and water–methanol successive extraction were 22.7 and 7.0 µmol/g DW, respectively.

4. Conclusions

In this study, we investigated monthly variations in the composition of Usujiri dulse (*Devaleraea inkyuleei*, formerly *Palmaria palmata* in Japan) in 2021. Drawing also on our similar work in 2019–2020, we found that MAAs were best prepared from Usujiri dulse collected between the middle of February and late April. We also identified a possible new relationship between MAAs and floridean starch contents. However, some factors affecting MAA composition were still unclear after our three years of investigations. Further studies will contribute to a better understanding of algal composition and related environmental factors. Finally, we found that the most effective extraction method for MAAs involved the use of 25% ethanol. This information will be helpful for the extraction of MAAs in an environmentally friendly manner.

Supplementary Materials: The following supporting information can be downloaded at <https://www.mdpi.com/article/10.3390/phycology3010008/s1>: Figure S1: HPLC chromatogram of dulce crude MAA solution.

Author Contributions: Y.K. and H.K. conceived and designed the research; R.Y. performed the experiments; R.Y. and Y.M. analyzed the data; Y.K., M.A.M.M. and H.K. contributed to writing and editing the manuscript. All authors have read and agreed to the published version of the manuscript.

Funding: This research received no external funding.

Institutional Review Board Statement: Not applicable.

Informed Consent Statement: Not applicable.

Data Availability Statement: No new data were created or analyzed in this study.

Acknowledgments: We gratefully acknowledge the sampling assistants of *Devaleraea inkyuleei* in Usujiri, Japan: Hiroyuki Munehara, Atsuya Miyajima, and Chikara Kawagoe.

Conflicts of Interest: The authors declare no conflict of interest.

References

1. Suh, S.-S.; Hwang, J.; Park, M.; Seo, H.H.; Kim, H.-S.; Lee, J.H.; Moh, S.H.; Lee, T.-K. Anti-Inflammation Activities of Mycosporine-Like Amino Acids (MAAs) in Response to UV Radiation Suggest Potential Anti-Skin Aging Activity. *Mar. Drugs* **2014**, *12*, 5174–5187. [[CrossRef](#)] [[PubMed](#)]
2. Kim, S.Y.; Cho, W.K.; Kim, H.-I.; Paek, S.H.; Jang, S.J.; Jo, Y.; Choi, H.; Lee, J.H.; Moh, S.H. Transcriptome Profiling of Human Follicle Dermal Papilla Cells in response to Porphyrin-334 Treatment by RNA-Seq. *Evid. Based Complement. Alternat. Med.* **2021**, *2021*, 6637513. [[CrossRef](#)] [[PubMed](#)]
3. Vega, J.; Schneider, G.; Moreira, B.R.; Herrera, C.; Bonomi-Barufi, J.; Figueroa, F.L. Mycosporine-Like Amino Acids from Red Macroalgae: UV-Photoprotectors with Potential Cosmeceutical Applications. *Appl. Sci.* **2021**, *11*, 5112. [[CrossRef](#)]
4. Rosic, N.N. Recent advances in the discovery of novel marine natural products and mycosporine-like amino acid UV-absorbing compounds. *Appl. Microbiol. Biotechnol.* **2021**, *105*, 7053–7067. [[CrossRef](#)]
5. Ryu, J.; Park, S.-J.; Kim, I.-H.; Choi Hee, Y.; Nam, T.-J. Protective effect of porphyrin-334 on UVA-induced photoaging in human skin fibroblasts. *Int. J. Mol. Med.* **2014**, *34*, 796–803. [[CrossRef](#)] [[PubMed](#)]
6. Orfanoudaki, M.; Hartmann, A.; Alilou, M.; Gelbrich, T.; Planchenault, P.; Derbré, S.; Schinkovitz, A.; Richomme, P.; Hensel, A.; Ganzera, M. Absolute Configuration of Mycosporine-Like Amino Acids, Their Wound Healing Properties and In Vitro Anti-Aging Effects. *Mar. Drugs* **2020**, *18*, 35. [[CrossRef](#)]
7. Lawrence, K.P.; Gacesa, R.; Long, P.F.; Young, A.R. Molecular photoprotection of human keratinocytes in vitro by the naturally occurring mycosporine-like amino acid palythine. *Br. J. Dermatol.* **2018**, *178*, 1353–1363. [[CrossRef](#)]
8. Danovaro, R.; Bongiorno, L.; Corinaldesi, C.; Giovannelli, D.; Damiani, E.; Astolfi, P.; Greci, L.; Pusceddu, A. Sunscreens Cause Coral Bleaching by Promoting Viral Infections. *Environ. Health Perspect.* **2008**, *116*, 441–447. [[CrossRef](#)]
9. Pangestuti, R.; Siahaan, E.A.; Kim, S.-K. Photoprotective Substances Derived from Marine Algae. *Mar. Drugs* **2018**, *16*, 399. [[CrossRef](#)]
10. Barnes, P.W.; Williamson, C.E.; Lucas, R.M.; Robinson, S.A.; Madronich, S.; Paul, N.D.; Bornman, J.F.; Bais, A.F.; Sulzberger, B.; Wilson, S.R.; et al. Ozone depletion, ultraviolet radiation, climate change and prospects for a sustainable future. *Nat. Sustain.* **2019**, *2*, 569–579. [[CrossRef](#)]
11. Núñez-Pons, L.; Avila, C.; Romano, G.; Verde, C.; Giordano, D. UV-Protective Compounds in Marine Organisms from the Southern Ocean. *Mar. Drugs* **2018**, *16*, 336. [[CrossRef](#)] [[PubMed](#)]
12. Álvarez-Gómez, F.; Korbee, N.; Casas-Arrojo, V.; Abdala-Díaz, R.T.; Figueroa, F.L. UV Photoprotection, Cytotoxicity and Immunology Capacity of Red Algae Extracts. *Molecules* **2019**, *24*, 341. [[CrossRef](#)] [[PubMed](#)]
13. Bonomi-Barufi, J.; Figueroa, F.L.; Korbee, N.; Momoli, M.M.; Martins, A.P.; Colepicolo, P.; Van Sluys, M.-A.; Oliveira, M.C. How macroalgae can deal with radiation variability and photoacclimation capacity: The example of *Gracilaria tenuistipitata* (Rhodophyta) in laboratory. *Algal Res.* **2020**, *50*, 102007. [[CrossRef](#)]
14. Karentz, D.; McEuen, F.S.; Land, M.C.; Dunlap, W.C. Survey of mycosporine-like amino acid compounds in Antarctic marine organisms: Potential protection from ultraviolet exposure. *Mar. Biol.* **1991**, *108*, 157–166. [[CrossRef](#)]
15. Jain, S.; Prajapat, G.; Abrar, M.; Ledwani, L.; Singh, A.; Agrawal, A. Cyanobacteria as efficient producers of mycosporine-like amino acids. *J. Basic Microbiol.* **2017**, *57*, 715–727. [[CrossRef](#)]
16. Sinha, R.P.; Singh, S.P.; Häder, D.-P. Database on mycosporines and mycosporine-like amino acids (MAAs) in fungi, cyanobacteria, macroalgae, phytoplankton and animals. *J. Photochem. Photobiol. B Biol.* **2007**, *89*, 29–35. [[CrossRef](#)]
17. Geraldes, V.; Pinto, E. Mycosporine-Like Amino Acids (MAAs): Biology, Chemistry and Identification Features. *Pharmaceuticals* **2021**, *14*, 63. [[CrossRef](#)]

18. Karsten, U.; Sawall, T.; Wiencke, C. A survey of the distribution of UV-absorbing substances in tropical macroalgae. *Phycol. Res.* **1998**, *46*, 271–279. [[CrossRef](#)]
19. Chuang, L.F.; Chou, H.N.; Sung, P.J. Porphyrin-334 isolated from the marine algae *Bangia atropurpurea*: Conformational performance for energy conversion. *Mar. Drugs* **2014**, *12*, 4732–4740. [[CrossRef](#)]
20. Conde, F.R.; Carignan, M.O.; Churio, M.S.; Carreto, J.I. In Vitro cis–trans photoisomerization of palythene and usujirene. Implications on the in vivo transformation of mycosporine-like amino acids. *Photochem. Photobiol.* **2003**, *77*, 146–150. [[CrossRef](#)]
21. Conde, F.R.; Churio, M.S.; Previtali, C.M. The photoprotector mechanism of mycosporine-like amino acids. Excited-state properties and photostability of porphyrin-334 in aqueous solution. *J. Photochem. Photobiol. B Biol.* **2000**, *56*, 139–144. [[CrossRef](#)]
22. Torres, P.; Santos, J.; Chow, F.; Ferreira, M.J.P.; Santos, D. Comparative analysis of in vitro antioxidant capacities of mycosporine like amino acids (MAAs). *Algal Res.* **2018**, *34*, 57–67. [[CrossRef](#)]
23. Pallela, R.; Na-Young, Y.; Kim, S. Anti-photoaging and photoprotective compounds derived from marine organisms. *Mar. Drugs* **2010**, *8*, 1189–1202. [[CrossRef](#)]
24. Guillerme, J.-B.; Couteau, C.; Coiffard, L. Applications for marine resources in cosmetics. *Cosmetics* **2017**, *4*, 35. [[CrossRef](#)]
25. Korbee, N.; Huovinen, P.; Figueroa, F.L.; Aguilera, J.; Karsten, U. Availability of ammonium influences photosynthesis and the accumulation of mycosporine-like amino acids in two *Porphyrin* species (Bangiales, Rhodophyta). *Mar. Biol.* **2005**, *146*, 645–654. [[CrossRef](#)]
26. Jiang, H.; Gao, K.; Helbling, E.W. UV-absorbing compounds in *Porphyrin haitanensis* (Rhodophyta) with special reference to effects of desiccation. *Environ. Boil. Fishes* **2007**, *20*, 387–395. [[CrossRef](#)]
27. Carreto, J.I.; Carignan, M.O. Mycosporine-like amino acids: Relevant secondary metabolites. Chemical and ecological aspects. *Mar. Drugs* **2011**, *9*, 387–446. [[CrossRef](#)] [[PubMed](#)]
28. Briani, B.; Sissini, M.N.; Lucena, L.A.; Batista, M.B.; Costa, I.O.; Nunes, J.M.C.; Schmitz, C.; Ramlov, F.; Maraschin, M.; Korbee, N.; et al. The influence of environmental features in the content of mycosporine-like amino acids in red marine algae along the Brazilian coast. *J. Phycol.* **2018**, *54*, 380–390. [[CrossRef](#)]
29. Pliego-Cortés, H.; Bedoux, G.; Boulho, R.; Taupin, L.; Freile-Peigrín, Y.; Bourgoignon, N.; Robledo, D. Stress tolerance and photoadaptation to solar radiation in *Rhodymenia pseudopalmata* (Rhodophyta) through mycosporine-like amino acids, phenolic compounds, and pigments in an Integrated Multi-Trophic Aquaculture system. *Algal Res.* **2019**, *41*, 101542. [[CrossRef](#)]
30. Diehl, N.; Michalik, D.; Zuccarello, G.C.; Karsten, U. Stress metabolite pattern in the eulittoral red alga *Pyropia plicata* (Bangiales) in New Zealand—Mycosporine-like amino acids and heterosides. *J. Exp. Mar. Bio. Ecol.* **2019**, *510*, 23–30. [[CrossRef](#)]
31. Véliz, K.; Chandía, N.; Karsten, U.; Lara, C.; Thiel, M. Geographic variation in biochemical and physiological traits of the red seaweeds *Chondracanthus chamissoi* and *Gelidium linguatum* from the south east Pacific coast. *J. Appl. Phycol.* **2019**, *31*, 665–682. [[CrossRef](#)]
32. Klisch, M.; Sinha, R.P.; Richter, P.R.; Häder, D.-P. Mycosporine-like amino acids (MAAs) protect against UV-B-induced damage in *Gyrodinium dorsum* Kofoid. *J. Plant Physiol.* **2001**, *158*, 1449–1454. [[CrossRef](#)]
33. Oren, A.; Gunde-Cimerman, N. Mycosporines and mycosporine-like amino acids: UV protectants or multipurpose secondary metabolites? *FEMS Microbiol. Lett.* **2007**, *269*, 1–10. [[CrossRef](#)] [[PubMed](#)]
34. Rosic, N.N.; Dove, S. Mycosporine-Like Amino Acids from Coral Dinoflagellates. *Appl. Environ. Microbiol.* **2011**, *77*, 8478–8486. [[CrossRef](#)] [[PubMed](#)]
35. Rødde, R.S.H.; Vårum, K.M.; Larsen, B.A.; Mykkestad, S.M. Seasonal and geographical variation in the chemical composition of the red alga *Palmaria palmata* (L.) Kuntze. *Bot. Mar.* **2004**, *47*, 125–133. [[CrossRef](#)]
36. Orfanoudaki, M.; Hartmann, A.; Kamiya, M.; West, J.; Ganzera, M. Chemotaxonomic Study of *Bostrychia* spp. (Ceramiaceae, Rhodophyta) Based on Their Mycosporine-Like Amino Acid Content. *Molecules* **2020**, *25*, 3273. [[CrossRef](#)]
37. Skriptsova, A.V.; Suzuki, M.; Semenchenko, A.A. Morphological variation in Northwest Pacific *Devaleraea mollis* and description of *D. inkyuleei* sp. nov. (Palmariaaceae, Rhodophyta). *Phycologia* **2022**, *61*, 606–615. [[CrossRef](#)]
38. Nishida, Y.; Saburi, W.; Miyabe, Y.; Kishimura, H.; Kumagai, Y. Characterization of Antioxidant Activity of Heated Mycosporine-like Amino Acids from Red Alga Dulse *Palmaria palmata* in Japan. *Mar. Drugs* **2022**, *20*, 184. [[CrossRef](#)]
39. Sato, N.; Furuta, T.; Takeda, T.; Miyabe, Y.; Ura, K.; Takagi, Y.; Yasui, H.; Kumagai, Y.; Kishimura, H. Antioxidant activity of proteins extracted from red alga dulse harvested in Japan. *J. Food Biochem.* **2019**, *43*, e12709. [[CrossRef](#)]
40. Furuta, T.; Miyabe, Y.; Yasui, H.; Kinoshita, Y.; Kishimura, H. Angiotensin I converting enzyme inhibitory peptides derived from phycobiliproteins of dulse *Palmaria palmata*. *Mar. Drugs* **2016**, *14*, 32. [[CrossRef](#)]
41. Yamamoto, Y.; Kishimura, H.; Kinoshita, Y.; Saburi, W.; Kumagai, Y.; Yasui, H.; Ojima, T. Enzymatic production of xylooligosaccharides from red alga dulse (*Palmaria* sp.) wasted in Japan. *Process Biochem.* **2019**, *82*, 117–122. [[CrossRef](#)]
42. Kobayashi, M.; Kumagai, Y.; Yamamoto, Y.; Yasui, H.; Kishimura, H. Identification of a Key Enzyme for the Hydrolysis of β -(1-3)-Xylosyl Linkage in Red Alga Dulse Xylooligosaccharide from *Bifidobacterium adolescentis*. *Mar. Drugs* **2020**, *18*, 174. [[CrossRef](#)] [[PubMed](#)]
43. Kumagai, Y.; Miyabe, Y.; Takeda, T.; Adachi, K.; Yasui, H.; Kishimura, H. In Silico Analysis of Relationship between Proteins from Plastid Genome of Red Alga *Palmaria* sp. (Japan) and Angiotensin I Converting Enzyme Inhibitory Peptides. *Mar. Drugs* **2019**, *17*, 190. [[CrossRef](#)] [[PubMed](#)]

44. Kumagai, Y.; Tsubouchi, R.; Miyabe, Y.; Takeda, T.; Adachi, K.; Yasui, H.; Kishimura, H. Complete sequence of mitochondrial DNA of red alga dulce *Palmaria palmata* (Linnaeus) Weber & Mohr in Japan. *Mitochondrial DNA Part B* **2019**, *4*, 3177–3178. [[CrossRef](#)] [[PubMed](#)]
45. Miyabe, Y.; Furuta, T.; Takeda, T.; Kanno, G.; Shimizu, T.; Tanaka, Y.; Gai, Z.; Yasui, H.; Kishimura, H. Structural Properties of Phycoerythrin from Dulce *Palmaria palmata*. *J. Food Biochem.* **2017**, *4*, 12301. [[CrossRef](#)]
46. Nishida, Y.; Kumagai, Y.; Michiba, S.; Yasui, H.; Kishimura, H. Efficient Extraction and Antioxidant Capacity of Mycosporine-Like Amino Acids from Red Alga Dulce *Palmaria palmata* in Japan. *Mar. Drugs* **2020**, *18*, 502. [[CrossRef](#)] [[PubMed](#)]
47. Nishida, Y.; Miyabe, Y.; Kishimura, H.; Kumagai, Y. Monthly Variation and Ultraviolet Stability of Mycosporine-like Amino Acids from Red Alga Dulce *Palmaria palmata* in Japan. *Phycology* **2021**, *1*, 119–128. [[CrossRef](#)]
48. Beer, S.; Eshel, A. Determining phycoerythrin and phycocyanin concentrations in aqueous crude extracts of red algae. *Mar. Freshw. Res.* **1985**, *36*, 785–792. [[CrossRef](#)]
49. Ekman, P.; Yu, S.; Pedersen, M. Effects of altered salinity, darkness and algal nutrient status on floridoside and starch content, α -galactosidase activity and agar yield of cultivated *Gracilaria sordida*. *Br. Phycol. J.* **1991**, *26*, 123–131. [[CrossRef](#)]
50. Shick, J.M.; Romaine-Lioud, S.; Ferrier-Pages, C.; Gattuso, J.P. Ultraviolet-B radiation stimulates shikimate pathway-dependent accumulation of mycosporine-like amino acids in the coral *Stylophora pistillata* despite decreases in its population of symbiotic dinoflagellates. *Limnol. Oceanogr.* **1999**, *44*, 1667–1682. [[CrossRef](#)]
51. Bhatia, S.; Sharma, K.; Namdeo, A.G.; Chaugule, B.B.; Kavale, M.; Nanda, S. Broad-spectrum sun-protective action of Porphyra-334 derived from *Porphyra vietnamensis*. *Pharmacogn. Res.* **2010**, *2*, 45–49. [[CrossRef](#)]
52. Kudo, I.; Matsunaga, K. Environmental Factors Affecting the Occurrence and Production of the Spring Phytoplankton Bloom in Funka Bay, Japan. *J. Oceanogr.* **1999**, *55*, 505–513. [[CrossRef](#)]
53. Isada, T.; Hirawake, T.; Nakada, S.; Kobayashi, T.; Sasaki, K.; Tanaka, Y.; Watanabe, S.; Suzuki, K.; Saitoh, S.-I. Influence of hydrography on the spatiotemporal variability of phytoplankton assemblages and primary productivity in Funka Bay and the Tsugaru Strait. *Estuar. Coast. Shelf Sci.* **2017**, *188*, 199–211. [[CrossRef](#)]
54. Yuan, Y.V.; Westcott, N.D.; Hu, C.; Kitts, D.D. Mycosporine-like amino acid composition of the edible red alga, *Palmaria palmata* (dulce) harvested from the west and east coasts of Grand Manan Island, New Brunswick. *Food Chem.* **2009**, *112*, 321–328. [[CrossRef](#)]
55. Lalegerie, F.; Stiger-Pouvreau, V.; Connan, S. Temporal variation in pigment and mycosporine-like amino acid composition of the red macroalga *Palmaria palmata* from Brittany (France): Hypothesis on the MAA biosynthesis pathway under high irradiance. *J. Appl. Phycol.* **2020**, *32*, 2641–2656. [[CrossRef](#)]
56. Karsten, U.; Wiencke, C. Factors Controlling the Formation of UV-absorbing Mycosporine-like Amino Acids in the Marine Red Alga *Palmaria palmata* from Spitsbergen (Norway). *J. Plant Physiol.* **1999**, *155*, 407–415. [[CrossRef](#)]

Disclaimer/Publisher’s Note: The statements, opinions and data contained in all publications are solely those of the individual author(s) and contributor(s) and not of MDPI and/or the editor(s). MDPI and/or the editor(s) disclaim responsibility for any injury to people or property resulting from any ideas, methods, instructions or products referred to in the content.